Numerical Modeling of the Impact Response of Tidal Devices and Marine Mammals

Molly E. Grear#1, Michael R. Motley#2
#Civil and Environmental Engineering, University of Washington
Seattle WA USA
[1]mgrear@uw.edu
[2]mrmotley@uw.edu

***Abstract*—The potential effect of tidal devices on marine mammals is a concern for developing tidal energy resources worldwide. Expanding on work done by Pacific Northwest National Laboratory, Sandia National Laboratory, and the U.S. Department of Energy, this paper examines existing tissue data for the endangered Southern Resident Killer Whale *(Orcinus orca)* and the harbor seal *(Phoca vitulina)* to understand how variability in the data impacts the results. This paper describes methods for numerically characterizing marine mammal tissues and attempts to understand the impacts of the non-linear response and anisotropy present in most living tissue. An ABAQUS finite element model was created to characterize the response of the variability in material data and therefore elucidate data gaps in the biomechanical properties of marine mammals.**

***Index Terms*—Tidal energy, marine mammals, biomechanical tissue properties, fluid-structure interaction**

I. Introduction

Installing tidal devices poses a possible risk to marine mammals—a threat that could impede tidal energy development worldwide. Among the ways in which these devices can interfere with marine life is through blunt force impact, especially in the case of tidal turbines with rotating blades. Existing research in the area of marine mammal strike is primarily opportunistic and related to vessel strike. Deaths due to blunt force trauma, usually caused by vessel collision, are generally characterized by marine veterinarians' necropsies and catalogued [1] [2]. Observational reports also cover healing and scarring over the course of years for recovering animals that have undergone strike trauma [3] [2]. This empirical data lacks precise information about the forces involved in injuring the animal, so is difficult to apply to new tidal technology.

In some injury scenarios, marine mammal impact analysis has been used to inform regulation and best practice. Impact of a ship strike on a North Atlantic Right Whale *(Eubalaena glacialis)* mandible has been investigated through finite element modeling [4] [5]. The forces required to break the mandible were correlated with vessel speeds. To reduce deaths due to vessel strike, regulation of vessel speed in critical habitat was proposed. The forward velocity of tidal turbine blades is considerably lower than typical vessel speeds. Thus, the mechanism of injury likely to occur from tidal turbines is presumed to be dependent on tissue injury as opposed to bone injury. Studies have been conducted to understand the biomechanical tissue properties of marine mammals to reduce injury from tagging devices [6]. The Cuvier's beaked whale *(Ziphius cavirostris)* head tissues elastic moduli were tested at low stresses (<50 kPa) to understand the whales' sound reception mechanisms.

To fully understand the risks of tidal device impact, a complete understanding of marine mammal skin and blubber biomechanical properties is required. In marine mammals, the skin and blubber layers fulfill the role of protecting the inner structures of the animal, while also determining buoyancy, locomotion, drag, and heat retention. Typical biomechanical properties of marine mammals currently in the literature are limited to density, drag, heat capacity, and other properties that do not give a representation of the strength of the material. Material properties have been tested for various marine mammal species, but it is unknown how similar properties are between the species of cetaceans. Predicting injury from impact to the animal requires knowledge of the relationship between skin and blubber, the constitutive properties of the material, and the variation in these properties present in the population.

Recently, the Pacific Northwest National Laboratory (PNNL) and Sandia National Laboratory (SNL) undertook a preliminary analysis of a scenario with a Southern Resident Killer Whale (SRKW) and an open-centered horizontal axis tidal turbine [7]. Estimates using the same juvenile orca data presented later in this report showed primarily that the tissue data was too variable to make a definitive conclusion on the outcome. The turbine in the analysis was ducted, so the SRKW could not be hit at the tip of the blade; thus the reported blade speed represent the speed at the furthest point from the center where the whale could feasibly be struck. Modeling the blade at 1, 2, 3, 4 and 5 m/s with average data from the highly variable testing, the computational analysis predicted that tissue damage would occur in both the skin and blubber layers with blade speeds higher than 3 m/s. Blubber tissue damage was predicted at speeds higher than 2 m/s. The area of damage was progressively larger and deeper with higher speeds. Tissue damage was estimated by comparing the highest strain to the average strain to failure seen in the tissue testing data.

The skin and blubber of a SRKW are two distinct parts, with two different structures (Figure 1). Based on other mammal's dermal and hypodermal layers, it was hypothesized that the skin would be a stiffer outer layer, while the blubber would

be less stiff and have high extensibility. The skin would act as an elastic membrane, transmitting force, while the blubber absorbs it. Morphological studies of other mammals indicate that skin acts to resist the force of impact by transmitting force in tension in the skin layer, protecting underlying layers of fat, muscles, or organs [8]. Skin fulfills this important function by its ability to endure reversible deformation [9]. Skin behavior in response to trauma has been most thoroughly observed in human skin. One comparable example is with a projectile ten times the skin thickness in radius; the threshold velocity for breaking the skin was 4.6-5.2 m/s [10]. This behavior is also seen in multi-layered materials called 'sandwich composites'; a stiff outer layer allows the force to be spread and the internal material to absorb much of the energy [11]. The functionality is readily observable in human skin; often underlying layers bruise while the stiffer outer layer remains undamaged, allowing for less risk of infection or further damage while healing.

Fig. 1: Structure of juvenile killer whale skin and blubber.

In addition, natural variability exists in the mechanical properties of any material, and is present even more so in living tissue. The material can vary in different locations on the animal, as well as between animals and based on age of the animal. Furthermore, determining mechanical properties of biological materials in inherently uncertain, as measuring the subject in vivo is typically unfeasible. Hydrodynamic studies of dolphin skin suggest that the skin of harbor porpoise (*Phocoena phocoena*) employs anisotropy to reduce drag [12]. Human and pig skin have long been recognized to be anisotropic; this knowledge is often used in surgery to make incisions in locations which will heal favorably [13]. Since the skin is pretensioned in a living animal, the direction with higher tension is the stronger axis and incisions made parallel to that axis will heal faster. In the perpendicular direction, the wound tends to pull open based on the skin's natural tension. The abundance of data on terrestrial mammal's skin anisotropy suggests that SRKW skin would be anisotropic as well.

The literature data confirms that living tissue is a complicated material, which must be modeled accurately to accurately predict the result of a tidal turbine strike. To that end, the PNNL analysis described above was limited by the use of a simplified isotropic, hyperelastic model for whale tissues as well as the high level uncertainty in both the quality of tissue data and the predicted biomechanical properties. This paper presents recent work where the biomechanical tissue data was reexamined, a series of more complex, realistic tissue models were created, and a simpler finite element model was built to evaluate data gaps and compare each tissue model.

II. Tissue Modeling and Analysis

A. Tensile Tissue Testing

Existing biomechanical data of two SRKWs' and one harbor seal skin and blubber tissue was analyzed to understand the potential effects of tissue degradation, natural variability, and material anisotropy on the finite element modeling outcome. All three of these datasets were tested at the University of Washington's Friday Harbor Laboratories. Each animal specimen was frozen prior to testing. The data used in this study was based on samples of orca tissue taken from the top of the head of two SRKW, aged 0 months (a stillborn neonate) and 3 years (juvenile). The seal was an adult (exact age unknown) frozen for less than a month. Samples of the seal were taken from the neck and region between above the front flipper on each side of the seal.

For each specimen, tensile tests were performed on strips of skin using two shapes. The first shape was a dogbone shape used to ensure a failure in the middle of the strip and measure tensile strength of the material. The second was a straight strip of tissue, hereby called rectangular, and used to measure the elastic modulus (also called stiffness). For both configurations, the middle of the strip measured 7 mm. The width of specimen was measure in the middle to calculate the strength and elastic modulus. Both skin and blubber were tested using an MTS Synergie 100 using a 500 N load cell in tension. Samples were taken from the transverse (0°), longitudinal (90°), and diagonal (45°) directions. Tests were run at two strain rates, 1 mm/s and 10 mm/s. Poisson's ratio was estimated with an extensometer during tensile testing on additional neonate samples.

During each set of testing, the condition of the animal was recorded. The tissue was reportedly 'moderately decomposed' at the time of collection, as indicated by the necropsy [14]; the juvenile sample had been frozen prior to testing for approximately 1 year. The skin tissue was noticeably degraded in places, likely due to scraping on the sand as the whale washed ashore. In some patches, the outer layer of the skin was sloughing off and would separate from the rest of tissue. The effect of freezing and testing ex vivo are unknown.

Anisotropy and variability of the data were analyzed using the programming language R. Datasets were compared using a Welch Two Sample t-test. A Welch's Two Sample t-test tests the hypothesis that two means are equal and is appropriate when the two samples have unequal sample sizes and unequal variance. The test defines the statistic t using the formula:

$$t = \frac{\overline{X}_1 - \overline{X}_2}{\sqrt{\frac{s_1^2}{N_1} + \frac{s_2^2}{N_2}}} \quad (1)$$

$\overline{X}_1$, s_1^2 and $N_1$are the first sample's mean, variance, and sample size respectively. The degrees of freedom, df, are calculated with the following equation:

$$df = \frac{\left(\frac{s_1^2}{N_1} + \frac{s_2^2}{N_2}\right)^2}{\frac{s_1^4}{N_1^2\nu_1} + \frac{s_2^4}{N_2^2\nu_2}} \quad (2)$$

The p-value is then calculated using a two-tailed test using a t-table. The p-value predicts the probability that one would obtain the results observed if the two samples had the same mean. In this analysis, two sample t-tests that have a p-value of 0.05 or less will be considered significantly different; in that case, the null hypothesis that the two sample means are the same will be rejected.

B. Tissue Analysis

Two datasets of SRKW skin and blubber (a three-year old juvenile specimen and a neonate) showed different patterns. It is unknown whether the differences in patterns are based on the development of the animal or the degraded nature of the juvenile tissue. A third dataset of an adult harbor seal was analyzed for comparison. This analysis primarily focuses on the juvenile orca data, based on addressing the high variability noted in the PNNL report. The other two datasets are used chiefly to contextualize patterns seen in the juvenile data.

Each set of tensile testing data contained a small number of samples; the original size of the material obtained for testing was the limiting factor. Limited sample sizes produced a wide variability in each set. For example, with just 8 samples of blubber and skin, the skin and blubber elastic modulus results are not statistically different (p-value = 0.19, Figure 2), even though the properties observed under the microscope (Figure 1) seemed to be different. When comparing the two sets of stress strain curves for the blubber and skin, the two sets of data have a similar strain to failure and general appearance of the curves (Figure 3). In the case of the juvenile data, the skin shows a higher strain to failure than the blubber, unlike what was predicted based on other mammals. As shown in Figure 2 and Figure 3, the blubber has a higher variability than the skin.

The neonate data, on the other hand, shows all the predicted behaviors. The skin is much stiffer than the underlying blubber layer (p-value$<$0.001, Figure 4) and the two sets of responses do not look similar (Figure 5).

The orca data was definitively non-isotropic, showing a higher elastic modulus for all skin testing in the 90° direction than the 0° (Figure 6). For both the juvenile and neonate samples, the elastic modulus was significantly higher (p-value$<$0.001 and p-value = 0.002 respectively). A comparison of averages for the juvenile skin is shown in Figure 6.

Dogbone shaped samples were used to collect tensile strength data from each specimen. The results of strength testing showed similar variability, with the average juvenile 90° skin strength of 2.23 $\pm$ 0.86 MPa and 0° skin strength of 1.30 $\pm$ 0.95 MPa. The results for the neonatal orca exhibited the same patterns, in which the 90° data had a higher strength than the 0° data (1.72 and 1.21 MPa respectively).

The set of seal data showed the skin elastic modulus significantly higher than the blubber (p-value$<$0.001), but did not show a significant difference between the 0° and 90° elastic modulus data (p-value = 0.83). In testing for strength, a higher strength was shown for the 0° data than the 90° data (17.0 and 13.5 MPa respectively). The seal skin data was much

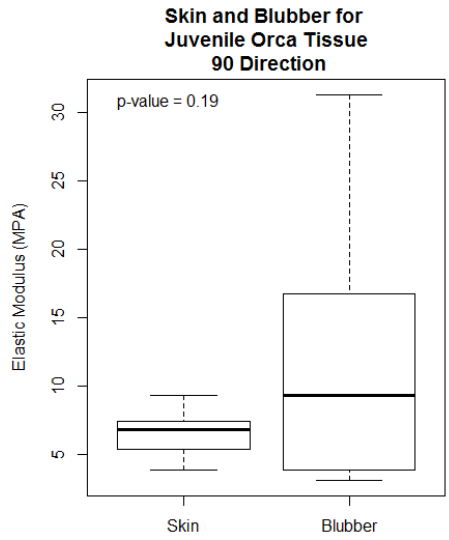

Fig. 2: Juvenile orca skin tissue and blubber tissue sampled in the 90° direction for the elastic modulus in tension. Box plot represents the means for 8 samples of each tissue. All tests were run at a strain rate of 1 mm/s.

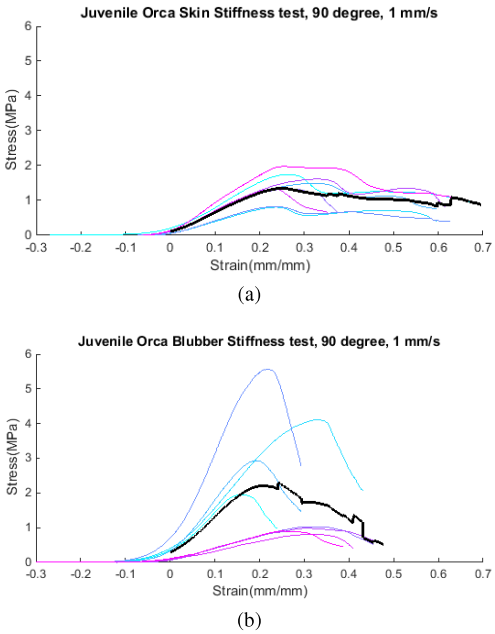

Fig. 3: Stress v. Strain curves for juvenile orca skin (a) and blubber (b) tissue sampled in the 90° direction for the elastic modulus in tension. All tests were run at a strain rate of 1mm/s. Black line represents an average created by adding all the responses together.

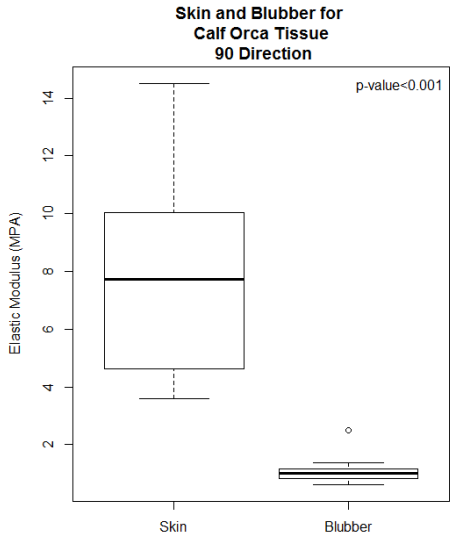

Fig. 4: Neonate orca skin tissue and blubber tissue sampled in the 90° direction for the elastic modulus in tension. Box plot represents the means for 11 samples of skin and 9 samples of blubber. All tests were run at a strain rate of 1 mm/s

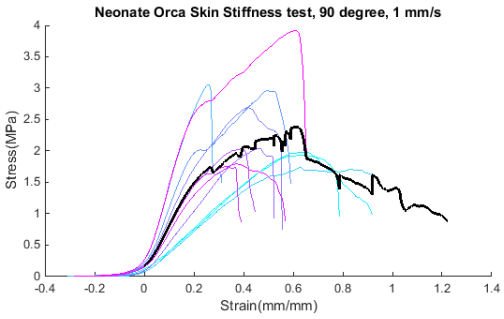

(a)

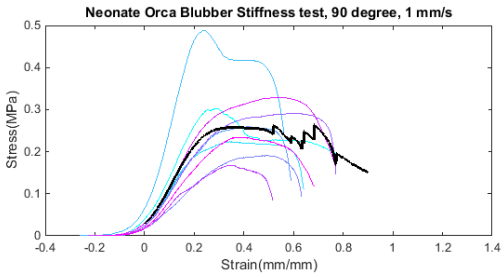

(b)

Fig. 5: Stress v. Strain curves for neonate orca skin (a) and blubber (b) tissue sampled in the 90° direction for the elastic modulus in tension. All tests were run at a strain rate of 1mm/s. Black line represents an average created by adding all the responses together. Note that the two plots have different y-axis scales since the response was quite different.

stiffer and stronger than the orca data.

Poisson's ratio was estimated using an extensometer test

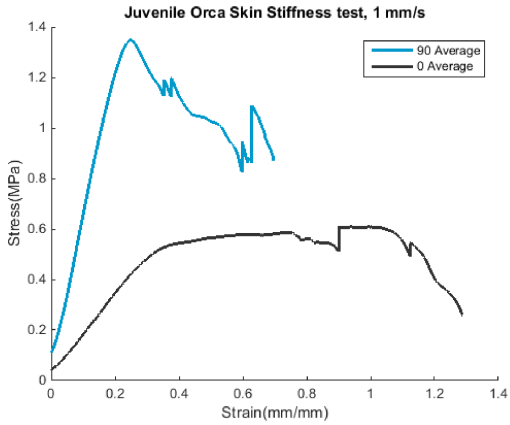

Fig. 6: The raw stress/strain curve for each sample of juvenile orca skin tissue sampled in the 90° and 0° directions were averaged. The 90° samples have a higher elastic modulus, but lower extensibility.

during the neonate skin testing. The value was estimated to be 0.47, which is consistent with literature values for similar materials.

For each set of data, the statistical power was low; thus, many material properties were considered to bound the results of this study.

III. Finite Element Modeling and Analysis

A. Model Setup

A finite element model was created using the commercial solver ABAQUS. A series of finite element models using the range of juvenile material properties was developed. Because the juvenile animal is behaviorally most at risk [7], this data was used to model the variability in impact response due to skin and blubber material parameter uncertainty. A parametric study was set up, where 9 runs were tested using high, low, and average values for the skin and blubber elastic modulus (Table I). For the blubber, there was one very high outlier (Figure 2), and in that case the second highest value was used.

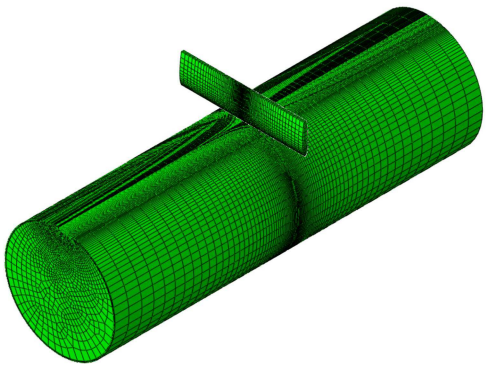

Fig. 7: Geometry of each model run.

A NACA 0015 airfoil geometry was used to model the blade as a general stand-in for a typical turbine blade. The blade is

TABLE I: SRKW Juvenile biomechanical skin and blubber elastic modulus properties used in ABAQUS modeling.

	Elastic Modulus (MPa)		
	Average	High	Low
Blubber	11.80	17.94	3.16
Skin	6.60	9.36	3.90

based on a 6 meter diameter turbine, similar to that modeled in the PNNL report [7]. The width of the blade is modeled as 10% of the blade's length. The blade's material properties were modeled as steel for simplicity (Table II), with linear elastic material properties. A cylinder was used as a simplified model of the animal (Figure 7), based on the girth of an average-sized SRKW, at 90 cm in diameter. The skin thickness in the circular model is the average of the juvenile SRKW skin sample thicknesses. The density of the whale was modeled as 1000 kg/m^3 in the absence of specific orca density data. Literature data shows that other marine mammals' skin and blubber have a similar range, with harp seal blubber at 920 $\pm$ 10 kg/m^3 [15], skin for a bottlenose dolphin at 969 $\pm$ 25 kg/m^3 [16], and skin for a manatee at 1,121 $\pm$ 42 kg/m^3 [16]. Poisson's ratio was input as 0.47 for both blubber and skin based on extensometer testing on the neonate skin.

TABLE II: Skin, Blubber, and Steel material properties used in ABAQUS modeling.

	Density (kg/m^3)	Poisson's Ratio	Elastic Modulus
Blubber	1000	0.47	*see Table I*
Skin	1000	0.47	*see Table I*
Blade	7750	0.3	200 GPa

Each set of material properties used 90° (nose to tail) data in an isotropic elastic model. Because the blade hits the animal perpendicularly to this direction in the proposed scenario, this value is more accurate for the analysis than the 0° (circumferential) data.

The ABAQUS model used 8-node reduced integration brick (C3D8R) elements, with a concentrated mesh in areas of interest. Mesh refinement studies were performed but are not shown here for brevity. The blade was given an initial velocity of 1 m/s. This represents an appropriate midspan blade forward velocity for a 12 m diameter blade. The whale model was given no boundary conditions and allowed to translate freely when hit by the blade.

IV. Finite Element Model Results

The parametric study was run for each of the 9 cases. The average skin-average blubber was the baseline for this study. Von Mises Stress was calculated on the top center element of the whale skin model, directly under the blade; displacement was calculated on the corresponding node. The node and element represent the maximum stress and displacement present in the whale model in the center of the model, directly under the center of the blade. As shown in Figure 8a, the maximum stress in the skin exceeds the average tensile strength of 2.23 MPa. In Figure 8b, the gradual increase in displacement seen after the initial impact results from the whale translating downward after the blade impact. Thus, the critical displacement and corresponding stress corresponds to the peak values shown at approximately time $t = 0.025$ seconds.

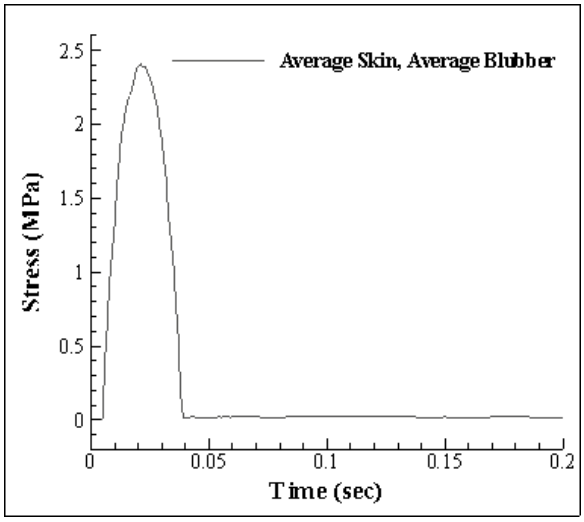

(a)

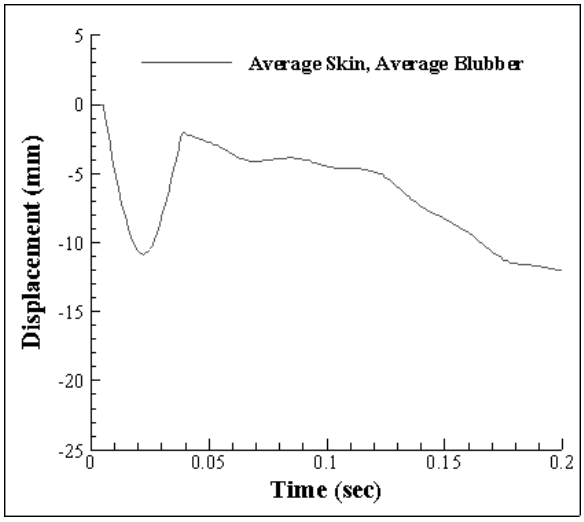

(b)

Fig. 8: Stress (a) and displacement (b) in juvenile orca skin directly under the blade is shown for a model run using average skin elastic modulus values and average blubber values.

While the average skin-average blubber model shows maximum stresses above the experimentally observed strength of the skin, the lower stiffness blubber values show scenarios where the skin does not reach the strength limit. In these cases, the skin's maximum stress response is similar, ranging from 1-1.5 MPa (Figure 9a). These maximum stress values are all well under the average tensile strength of 2.23 MPa measured

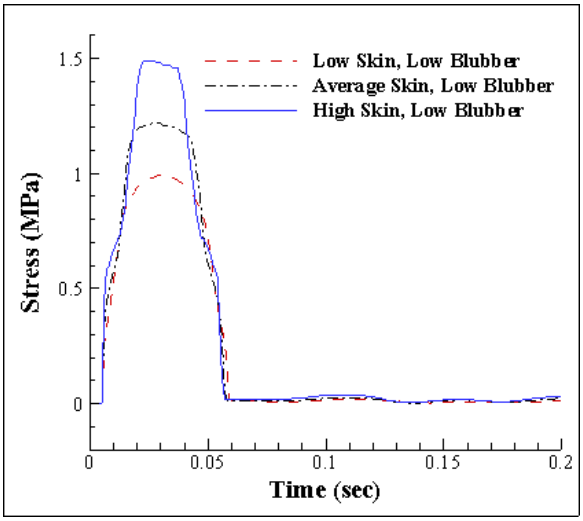

(a)

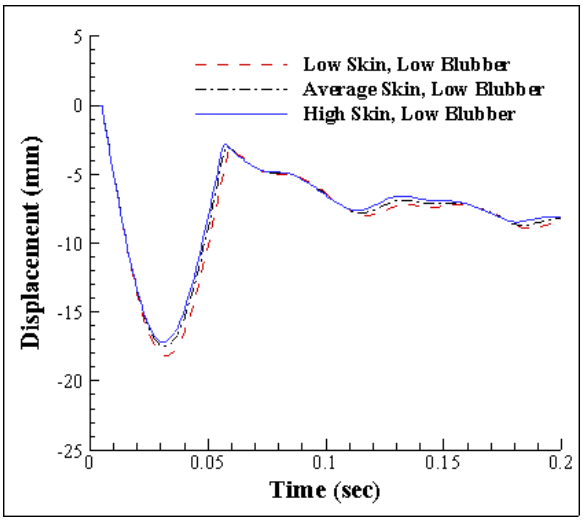

(b)

Fig. 9: Stress (a) and displacement (b) output using high (9.36 MPa), average (6.60 MPa), and low (3.90 MPa) juvenile orca skin data with low (3.16 MPa) juvenile orca blubber data. In Figure a., higher skin stiffness shows higher stress in the animal. Figure b. illustrates that high skin stiffness however does not cause much larger displacement response.

during tissue testing. As shown in Figure 9b, the variation in displacement corresponding to these maximum stress values in the skin is negligible. Figures 10a-c show contour plots of the von Mises stresses and displacements directly beneath the blade at the point of impact. In these figures, the maximum stress contour is set to 2.23 MPa, the experimentally observed tensile strength of the skin. As a result, it is evident that only a very small region in the skin in Figure 10c exceeds this average tensile strength, as denoted by the white region in the figure. This suggests that in these scenarios, the animal would only incur damage to the skin in the case of high skin-low blubber. The location of the maximum stress is at the interface

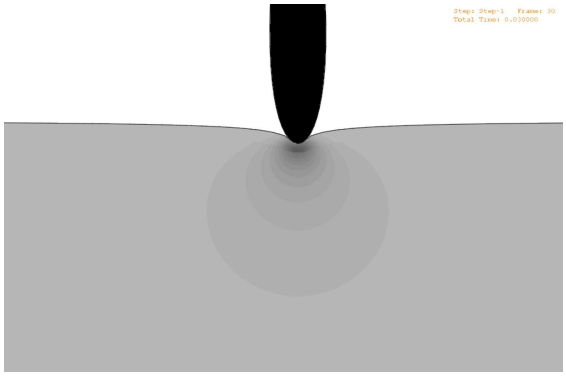

(a) Low Skin, Low Blubber

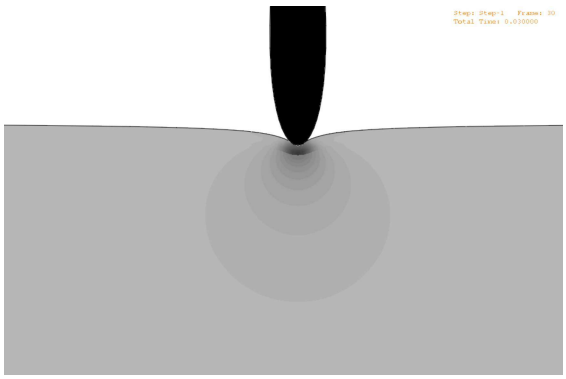

(b) Average Skin, Low Blubber

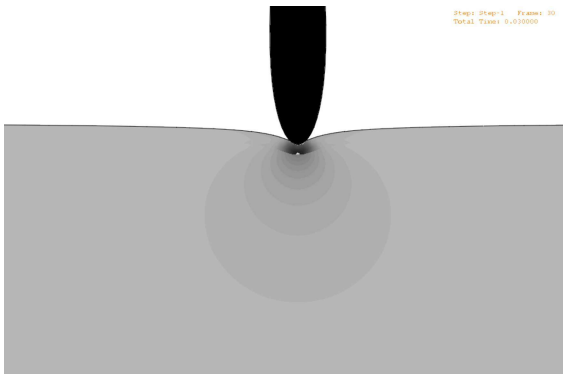

(c) High Skin, Low Blubber

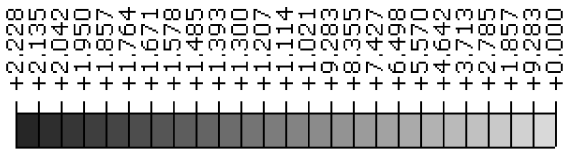

Fig. 10: By varying the skin elastic modulus, using low (Fig. a, 3.90 MPa), average (Fig. b, 6.60 MPa), and high (Fig. c, 9.36 MPa) values, and holding the blubber elastic modulus constant, at low (3.16 MPa) value, differences between each set of material models are shown. Data are displayed at the time of maximum stress (0.03 s). The maximum stress value (shown in darkest gray) is set to 2.23 MPa, the averaged maximum tensile strength of skin. Areas of white (seen in Fig. c) represent regions where the stress exceeds the tensile strength and therefore where skin would experience damage. Higher skin elastic modulus leads to more damage in the skin, but less damage to the underlying layers. Blade is in black.

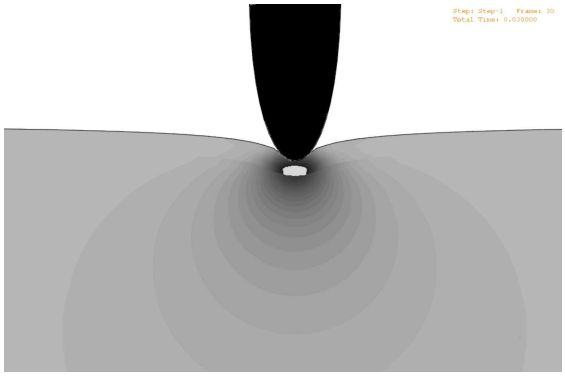

(a) Low Skin, Low Blubber

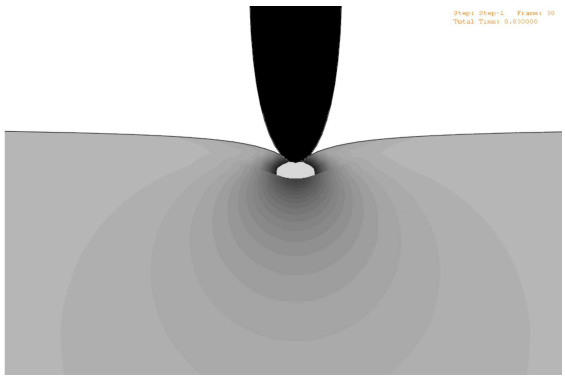

(b) Average Skin, Low Blubber

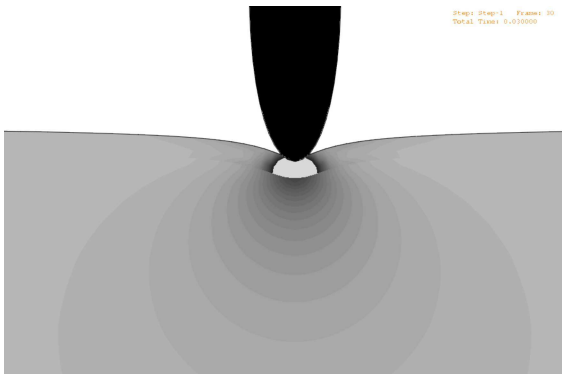

(c) High Skin, Low Blubber

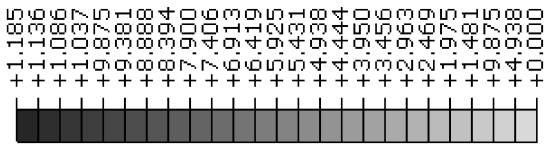

Fig. 11: Areas of white represent regions where the stress exceeds the average blubber tensile strength. In this case, the areas of white are not present in the blubber layer, so the blubber layer would not be damaged in any of these cases. The skin elastic modulus was varied from low (Fig. a, 3.90 MPa), average (Fig. b, 6.60 MPa), and high (Fig. c, 9.36 MPa), while the blubber elastic modulus was held constant, at low (3.16 MPa) value. Data are displayed at the time of maximum stress (0.03 s). Higher skin stiffness is shown to lead to lower blubber stresses. The maximum stress value (shown in darkest gray) is set to 1.19 MPa, the maximum blubber tensile strength. Blade is in black.

between the blubber and skin, indicating the skin would likely not fail at the surface.

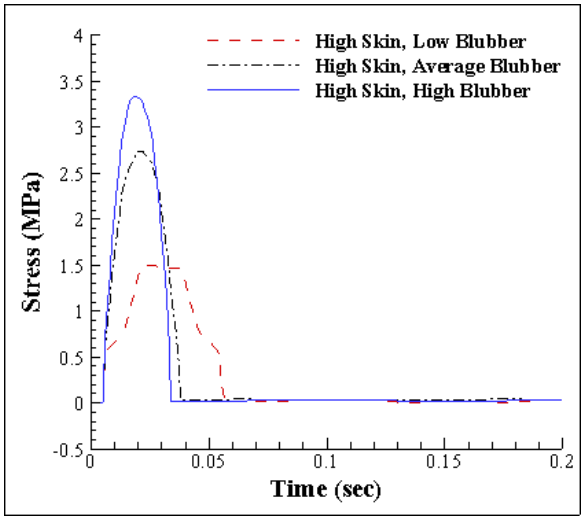

(a)

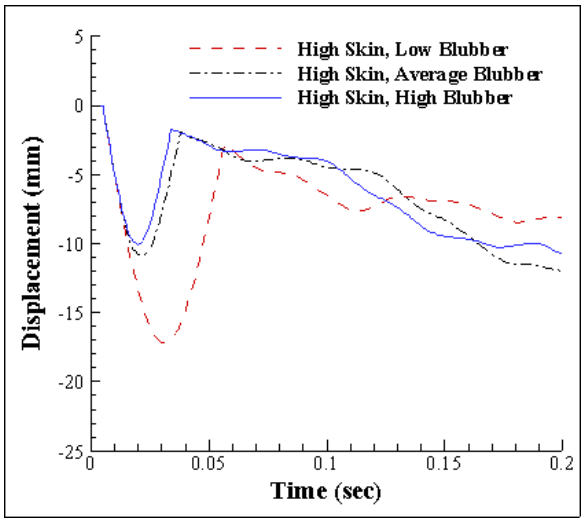

(b)

Fig. 12: Stress (a) and displacement (b) output using high (17.94 MPa), average (11.80 MPa), and low (3.16 MPa) juvenile orca blubber data with high (9.36 MPa) juvenile orca skin data. The maximum stress is shown here as the element with the maximum stress, in the center of the animal directly under the blade. The maximum displacement is shown from the corresponding node.

Figure 11 shows the same analysis as in Figure 10, but this time with the blubber's maximum tensile strength (in the 90° direction), 1.19 ± 0.67 MPa, set as the maximum value in the legend to highlight where the blubber layer would receive damage. When the maximum stress shown was set to the blubber's average tensile strength, the results also show that the blubber is unlikely to fail (Figure 11). The low blubber values were most like what was hypothesized and seen in other tissue testing. The blubber stress decreases as the skin stress

increases, suggesting that the stiffer skin is acting to spread the force when stiffer than the blubber.

In contrast, a comparison of a range of extreme blubber values while holding the skin value constant leads to markedly different results. Figure 12a shows that increasing the blubber elastic modulus value greatly increases the stress present in the skin. Correspondingly, the displacements show a similar trend, with the greatest displacement corresponding to the lowest value for blubber's elastic modulus (Figure 12b). For the high and average blubber elastic modulus values, large regions of the skin and blubber fail, indicating the animal retains some injury. Figure 13 shows that the average tensile strength is exceeded for all cases in the skin. The blubber's tensile strength is exceeded in the case of average blubber and high blubber.

For the remaining models, areas of the skin and blubber reached the maximum tensile strength, indicating that the SRKW retained some injury.

V. Discussion and Conclusions

The relationships between the skin and blubber for the juvenile SRKW were explored in depth. Harbor seal and a neonate SRKW were analyzed for comparison. The SRKW juvenile tensile testing showed blubber elastic modulus was an average of 1.8 times higher than that of its skin in the nose to tail direction. The neonate testing exhibited skin that was approximately 8 times stiffer than the blubber in the same direction. The harbor seal skin layer data shows much stiffer and stronger patterns than the other sets of orca data, with the skin reporting elastic modulus properties approximately 43 times higher than the blubber. The seal skin's addition of fur that extends into the skin layer may contribute to the added stiffness. Patterns observed in the juvenile tensile testing contradictory to both the seal and SRKW neonate could be based on the aging of the animal, natural variation in the population, or degradation.

Juvenile SRKW stiffness data showed a large variability, which resulted in a spread of possible outcomes from no injury to the animal to significant tissue failure throughout the skin and into the blubber layer. This work is unable to comment on the types of injury sustained by the animal, as the material exceeding the yield strength likely results in a considerable amount of plastic deformation before fully breaking.

The 1 m/s blade speed represented a likely blade speed, but higher blade speeds would likely result in the same patterns, with more damage seen to both the skin and the blubber. To evaluate a specific turbine design, a more specific speed and geometry will be required.

This study aimed to bound the potential response of a turbine impact on an SRKW by evaluating a range of material properties. It is evident that the large variability created a spread of responses to large to have confidence in the impact result. Five out of nine model runs indicated the SRKW would incur an injury from the blade. The spread of potential injury ranged from no injury to the other extreme of tissue yielding throughout the skin layer and further into the blubber.

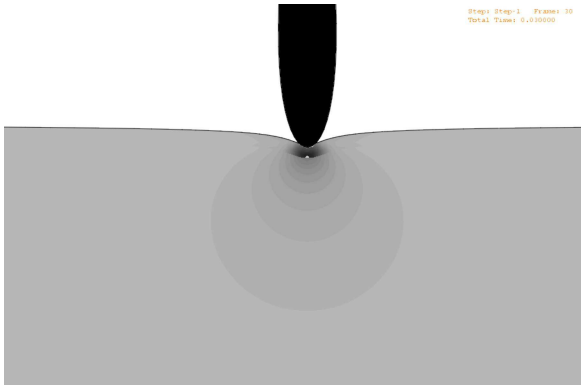

(a) High Skin, Low Blubber

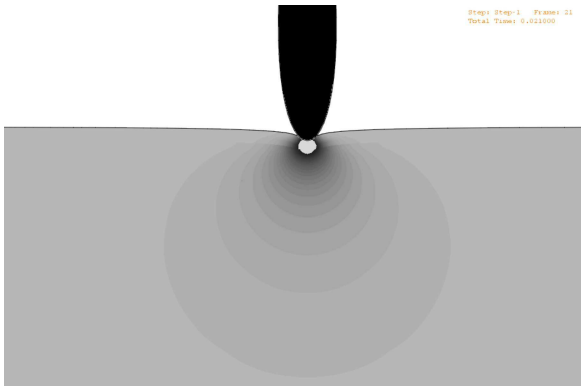

(b) High Skin, Average Blubber

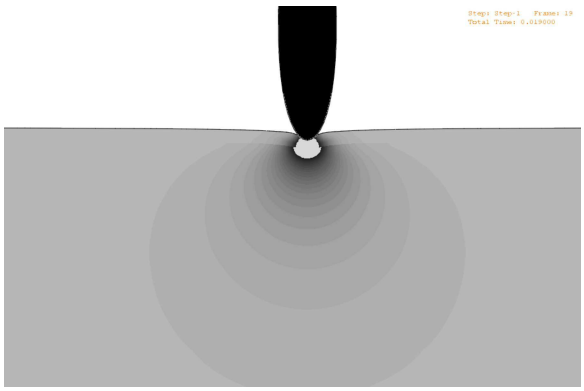

(c) High Skin, High Blubber

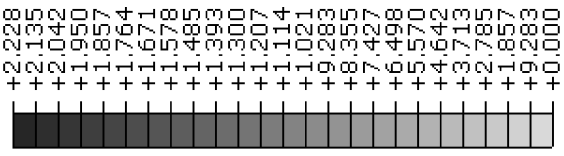

Fig. 13: Varying the blubber layer's material properties while holding the skin's properties constant is shown above. The blubber's elastic modulus was varied between low (Fig. a, 3.16 MPa), average (Fig. b, 11.80 MPa), and high (Fig c. 17.94 MPa) values, while the skin elastic modulus data was kept at a constant high value of 9.36 MPa. The three sets of data, shown at the time of maximum stress (0.02-0.03 s), illustrate that higher blubber stiffness leads to much higher stresses in the the skin. The maximum value (shown in darkest gray) is set to to 2.23 MPa, the experimental maximum strength of skin. Areas of white represent regions where the stress exceeds the blubber tensile strength. Blade is in black

VI. Future Work

Further investigations will include modeling of the bone in the animal, as well as a range of speeds for blade to further bound the potential outcome. The juvenile SRKW data showed the most variability, with the largest standard deviations and lowest sample size of all the data. The higher variability in the blubber stiffness data than the skin could suggest that degradation (as described in the necropsy report [14] and observed during testing), has a greater effect on blubber than skin. Combined with the fact that this sample was frozen for about a year, while the other samples were frozen less than 6 weeks, this dataset may be showing more variability than would expected in vivo. The variability of the responses shown in the numerical results describes a need for more testing to have confidence in modeling tissue properties of an SRKW. Tissue testing for SRKW, harbor seal, and harbor porpoise is ongoing and will contribute significantly to the confidence of these results. Testing of a harbor porpoise can likely bridge the understanding between patterns seen in the SRKW and harbor seal. Harbor porpoise is more closely related genetically to the SRKW as they are both cetaceans, whereas the harbor seal is a pinniped. Investigating the seal tissue under a microscope can show the structure of the seal fur and potentially describe the stiffer patterns seen in the seal skin. Experimental procedures in which tissue is tested before and after freezing can further illuminate effects of degradation on blubber and skin.

Additionally, much of the blubber region was found to be in compression during the model run. Currently, the model assumes a linear relationship between the material in tension and compression. Since blubber does not have much strength in tension, it is possible that the compressive strength and stiffness is considerably different. Compressive tests of blubber would be a valuable addition to understanding this topic. Given that the blubber does not hold it's shape when it is unrestrained, it is possible that the compressive stiffness may not be representative of the true material properties.

Extending the modeling work to a more realistic geometry to properly represent a whale (or other marine mammal) instead of a simplified cylindrical model can provide an additional layer of confidence. The model can be expanded to use anisotropic data, as well as strain rate data. Improving the material to include plastic regions based on the full stress strain curves will be further explored. With a more complicated model, the necessity for additional layers of complexity can be weighed.

Finally, this analysis can be combined with behavioral models of marine mammals currently underway. Behavioral data can predict the likelihood of encounter, as well as the potential population level repercussions of taking an animal. The layering of these two datasets provides a pathway to interpret the full picture of a tidal devices potential consequence on marine mammals. Together this data can inform regulatory decision making for permitting tidal devices.

Acknowledgment

This research was funded by the National Science Foundation's Graduate Research Fellowship Program. The foundation for this work, including all tissue testing, was funded by the U.S. Department of Energy, and conceived through joint efforts of the U.S. Department of Energy (DOE), the National Oceanic and Atmospheric Administration (NOAA), Snohomish County Public Utility District (SnoPUD), OpenHydro Group Limited, the University of Washington - Northwest National Marine Renewable Energy Centre (UWNNMREC), Pacific Northwest National Laboratory (PNNL), and Sandia National Laboratories (SNL). This expanded tissue modeling effort would not be possible without the ongoing support from these partners. Drs. Adam Summers and Petra Ditsche (University of Washington) have lent their expertise in comparative biomechanics and laboratory testing.

References

[1] R. Campbell-Malone, S. Barco, P.-Y. Daous, A. Knowlton, W. McLellan, D. Rotstein, and M. Moore, "Gross and histologic evidence of sharp and blunt trauma in north atlantic right whales (*Eubalaena glacialis*) killed by ships." *Journal of Zoo and Wildlife Medicine*, vol. 39, no. 1, pp. 37–55, 2008.

[2] A. S. Jensen and G. K. Silber, "Large whale ship strike database," NOAA Technical Memorandum NMFS-OPR-25, U.S. Department of Commerce, Washington, D.C., USA, Tech. Rep., 2004.

[3] I. N. Visser, "Propeller scars on and known home range of two orca (*Orcinus orca*) in New Zealand waters," *New Zealand Journal of Marine and Freshwater Research*, vol. 33, no. 4, pp. 635–642, 1999.

[4] R. Campbell-Malone, "Biomechanics of north atlantic right whale bone: Mandibular fracture as a fatal endpoint for blunt vessel-whale collision modeling." Ph.D. dissertation, Massachussetts Institute of Technology, 2007.

[5] I. Tsukrov, J. C. DeCew, K. Baldwin, R. Campbell-Malone, and M. J. Moore, "Mechanics of the right whale mandible: Full scale testing and finite element analysis," *Journal of Experimental Marine Biology and Ecology*, vol. 374, no. 2, pp. 93 – 103, 2009. [Online]. Available: http://www.sciencedirect.com/science/article/pii/S0022098109001014

[6] M. B. Hanson, "An evaluation of the relationship between small cetacean tag design and attachment durations: A bioengineering approach." Ph.D. dissertation, University of Washington, 2001.

[7] T. Carlson, M. Grear, A. Copping, M. Halvorsen, R. Jepsen, and K. Metzinger, "Assessment of strike of adult killer whales by an OpenHydro tidal turbine blade," *Report by Pacific Northwest National Laboratory (PNNL)*, p. pp 124, 2014.

[8] D. A. Danielson, "Human skin as an elastic membrane," *J. Biomechanics*, vol. 6, pp. 539–546, 1973.

[9] M. Pawlaczyk, M. Lelonkiewicz, and M. Wieczorowski, "Age-dependent biomechanical properties of the skin," *Advances in Dermatology and Allergology*, vol. 30, no. 5, p. 302306, 2013.

[10] M. Ali, V. Singh, and G. Parrey, "Rupture of human skin membrane under impact of parabolodial projectile: Bullet wound ballistics," *Defence Science Journal*, vol. 46, no. 4, 2013. [Online]. Available: http://publications.drdo.gov.in/ojs/index.php/dsj/article/view/4082

[11] T. Anderson and E. Madenci, "Experimental investigation of low-velocity impact characteristics of sandwich composites," *Composite Structures*, vol. 50, no. 3, pp. 239 – 247, 2000. [Online]. Available: http://www.sciencedirect.com/science/article/pii/S0263822300000982

[12] V. V. Pavlov, "Dolphin skin as a natural anisotropic compliant wall," *Bioinspiration and Biomemetics*, vol. 1, pp. 31–40, 2006.

[13] A. N. Annaidh, K. Bruyere, M. Destrade, M. D. Gilchrist, and M. Ottenio, "Characterising the Anisotropic Mechanical Properties of Excised Human Skin," *ArXiv e-prints*, Feb. 2013.

[14] D. D. J. Huggins and D. Lambourn, "Examination of dead killer whale on Long Beach Peninsula, February 12, 2012," Cascadia Research Collective, Tech. Rep., 2012. [Online]. Available: http://www.cascadiaresearch.org/examination_of_dead_killer_whale-12Feb2012.htm

[15] G. G. Beck and T. G. Smith, “Distribution of blubber in the northwest atlantic harp seal, phoca groenlandica,” *Canadian Journal of Zoology*, vol. 73, no. 11, pp. 1991–1998, 1995. [Online]. Available: http://dx.doi.org/10.1139/z95-234

[16] E. Kipps, W. McLellan, S. Rommel, and D. Pabst, “Skin density and its influence on buoyancy in the manatee, harbor porpoise, and bottlenose dolphin,” *Marine Mammal Science*, vol. 18, pp. 765–778, 07/02 2002. [Online]. Available: http://onlinelibrary.wiley.com/doi/10.1111/j.1748-7692.2002.tb01072.x/abstract